A Robust Control Approach for Underwater Vehicle Manipulator Systems in Interaction with Compliant Environments ⋆

Shahab Heshmati-alamdari * **Alexandros Nikou** **
Kostas J. Kyriakopoulos * **Dimos V. Dimarogonas** **

* *Control Systems Lab, Department of Mechanical Engineering, National Technical University of Athens, 9 Heroon Polytechniou Street, Zografou 15780.*
E-mail: {shahab, kkyria}@mail.ntua.gr
** *ACCESS Linnaeus Center, School of Electrical Engineering and KTH Center for Autonomous Systems, KTH Royal Institute of Technology, SE-100 44, Stockholm, Sweden.*
E-mail: {anikou, dimos}@kth.se

Abstract: In various interaction tasks using Underwater Vehicle Manipulator Systems (UVMSs) (e.g. sampling of the sea organisms, underwater welding), important factors such as: i) uncertainties and complexity of UVMS dynamic model ii) external disturbances (e.g. sea currents and waves) iii) imperfection and noises of measuring sensors iv) steady state performance as well as v) inferior overshoot of interaction force error, should be addressed during the force control design. Motivated by the above factors, this paper presents a model-free control protocol for force controlling of an Underwater Vehicle Manipulator System which is in contact with a compliant environment, without incorporating any knowledge of the UVMS's dynamic model, exogenous disturbances and sensor's noise model. Moreover, the transient and steady state response as well as reduction of overshooting force error are solely determined by certain designer-specified performance functions and are fully decoupled by the UVMS's dynamic model, the control gain selection, as well as the initial conditions. Finally, a simulation study clarifies the proposed method and verifies its efficiency.

Keywords: Underwater Vehicle Manipulator System, Nonlinear Control, Autonomous Underwater Vehicle, Marine Robotics, Force Control, Robust Control.

1. INTRODUCTION

In view of the development of autonomous underwater vehicles, the capability of such vehicles to interact with the environment by the use of a robot manipulator, had gained attention in the literature. Most of the underwater manipulation tasks, such as maintenance of ships, underwater pipeline or weld inspection, surveying, oil and gas searching, cable burial and mating of underwater connector, require the manipulator mounted on the vehicle to be in contact with the underwater object or environment. The aforementioned systems are complex and they are characterized by several strong constraints, namely the complexity in the mathematical model and the difficulty to control the vehicle. These constraints should be taken into consideration when designing a force control scheme. In order to increase the adaptability of UVMS, force control must be included into the control system of the UVMS. Although many force control schemes have been developed for earth-fixed manipulators and space robots, these control schemes cannot be used directly on UVMS because of the unstructured nature of the underwater environment.

From the control perspective, achieving these type of tasks requires specific approaches(Siciliano et al., 2009). However, speaking about underwater robotics, only few publications deal with the interaction control using UVMS. On the of the first underwater robotic setups for interaction with the environment was presented in (Casalino et al., 2001). Hybrid position/force control schemes for UVMS were developed and tested in (Clegg et al., 2001; Dunnigan et al., 1996). However, dynamic coupling between the manipulator and the underwater vehicle was not considered in the system model. In order to compensate the contact force, the authors in (Kajita and Kosuge, 1997) proposed a method that utilizes the restoring force generated by the thrusters. In the same context, position/force (Lapierre et al., 2003), impedance control (Cui et al., 1999; Cui and Sarkar, 2000; Cui and Yuh, 2003) and external force control schemes (Antonelli et al., 1999, 2002, 2001) can be found in the literature.

⋆ This work was supported by the ROBOCADEMY, Marie Curie ITN Grant Agreement no FP7-608096 funded by the EU action 7^{th} Framework Programme - The 2013 People Work Programme - EC Call Identifier FP7-PEOPLE- 2013-ITN, Implementation Mode: Multi-ITN

Over the last years, the interaction control of UVMS is gaining significant attention again. Several control issues for an UVMS in view of intervention tasks has been presented in (Marani et al., 2010). In (Cataldi and Antonelli, 2015) based on the interaction schemes presented in (Antonelli et al., 2001) and (Antonelli et al., 2002), the authors proposed a control protocol for turning valve scenarios. Recent study (Farivarnejad and Moosavian, 2014) proposed a multiple impedance control scheme for a dual manipulator mounted on AUV. Moreover, the two recent European projects TRIDENT(see, e.g. (Fernndez et al., 2013),(Prats et al., 2012),(Simetti et al., 2014)) and PANDORA (see, e.g. (Carrera et al., 2014), (Carrera et al., 2015)) have given boost to underwater interaction with relevant results.

In real applications, the UVMS needs to interact with the environment via its end-effector in order to achieve a desired task. During the manipulation process the following issues occur: the environment is potentially unknown, the system is in the presence of unknown (but bounded) external disturbances (sea currents and sea waves) and the sensor measurements are not always accurate (we have noise in the measurements). These issues can cause unpredicted instabilities to the system and need to be tackled during the control design. From the control design perspective, the UVMS dynamical model is highly nonlinear, complicated and has significant uncertainties. Owing to the aforementioned issues, underwater manipulation becomes a challenging task in order to achieve low overshoot, transient and steady state performance.

Motivated by the above, in this work we propose a force - position control scheme which does not require any knowledge of the UVMS dynamic parameters, environment model as well as the disturbances. More specifically, it tackles all the aforementioned issues and guarantees a predefined behavior of the system in terms of desired overshoot and prescribed transient/steady state performance. Moreover, noise measurements, UVMS model uncertainties (a challenging issue in underwater robotics) and external disturbance are considered during control design. In addition, the complexity of the proposed control law is significantly low. It is actually a static scheme involving only a few calculations to output the control signal, which enables its implementation on most of current UVMS. The rest of this paper is organized as follows: in Section 2 the mathematical model of UVMS and preliminary background are given. Section 3 provides the problem statement that we aim to solve in this paper. The control methodology is presented in Section 4. Section 5 validates our approach via a simulation study. Finally, conclusions and future work directions are discussed in Section 6.

2. PRELIMINARIES

2.1 Mathematical model of the UVMS

In this work, the vectors are denoted with lower bold letters whereas the matrices by capital bold letters. The end effector coordinates with respect to (w.r.t) the inertial frame $\{I\}$ are denoted by $\mathbf{x}_e \in \mathbb{R}^6$. Let $\mathbf{q} = [\mathbf{q}_a^\top,\ \mathbf{q}_m^\top]^\top \in \mathbb{R}^n$ be the state variables of the UVMS, where $\mathbf{q}_a = [\eta_1^\top, \eta_2^\top]^\top \in \mathbb{R}^6$ is the vector that involves the position vector η_1 and orientation η_2 of the vehicle w.r.t to the inertial frame $\{I\}$ and $\mathbf{q}_m \in \mathbb{R}^{n-6}$ is the vector of angular position of the manipulator's joints. Thus, we have (Antonelli, 2013; Fossen, 1994):

$$\dot{\mathbf{q}}_a = \mathbf{J}^a(\mathbf{q}_a)\mathbf{v} \tag{1}$$

where

$$\mathbf{J}^a(\mathbf{q}_a) = \begin{bmatrix} \mathbf{J}_t(\eta_2) & O_{(3\times3)} \\ O_{(3\times3)} & \mathbf{J}_r(\eta_2) \end{bmatrix} \in \mathbb{R}^{6\times6}$$

is the Jacobian matrix transforming the velocities from the body-fixed to the inertial frame and where, $\mathbf{0}_{3\times3}$ is the zero matrix of the respective dimensions, $\mathbf{v}_i$ is the vector of body velocities of the vehicle and $\mathbf{J}_t(\eta_2)$ and $\mathbf{J}_r(\eta_2)$ are the corresponding parts of the Jacobian related to position and orientation respectively. Moreover, for the augmented UVMS system the following forward kinematic equation holds(Antonelli, 2013):

$$\mathbf{x}_e = \mathbf{T}(\mathbf{q}) \tag{2}$$

where $\mathbf{x}_e = [{}^p\mathbf{x}_e, {}^o\mathbf{x}_e^\top]^\top \in \mathbb{R}^6$ denotes the coordinates of end-effector frame which include the vector of position ${}^p\mathbf{x}_e$ and orientation ${}^o\mathbf{x}_e$ of the end-effector. $\mathbf{T}(\cdot)$ is the homogeneous transformation matrix describing the position and orientation of the end-effector coordinates with reference to the inertial frame $\{I\}$. Eq. (2) yields (Antonelli, 2013):

$$\dot{\mathbf{x}}_e = \mathbf{J}(\mathbf{q})\boldsymbol{\zeta} \tag{3}$$

where $\boldsymbol{\zeta} = [\mathbf{v}^\top, \dot{\mathbf{q}}_m^\top]^\top$ is the velocity vector including the body velocities of the vehicle as well as the joint velocities of the manipulator and $\mathbf{J}(\mathbf{q})$ is the geometric Jacobian Matrix (Antonelli, 2013).

2.2 Dynamics

The dynamics of a UVMS using (1) and after some algebraic manipulations can be written as Antonelli (2013):

$$\bar{\mathbf{M}}(\mathbf{q})\ddot{\mathbf{q}} + \bar{\mathbf{C}}(\dot{\mathbf{q}},\mathbf{q})\dot{\mathbf{q}} + \bar{\mathbf{D}}(\dot{\mathbf{q}},\mathbf{q})\dot{\mathbf{q}} + \bar{\mathbf{g}}(\mathbf{q}) + \mathbf{J}^\top\boldsymbol{\lambda} + \boldsymbol{\delta}(t) = \boldsymbol{\tau} \tag{4}$$

where $\boldsymbol{\delta}(t)$ are bounded disturbances including system's uncertainties as well as the external disturbances affecting on the system from the environment (sea waves and currents), $\boldsymbol{\lambda} = [\mathbf{f}_e^\top, \boldsymbol{\nu}_e^\top]^\top$ the generalized vector including force $\mathbf{f}_e$ and torque $\boldsymbol{\nu}_e$ that the UVMS exerts on the environment at its end-effector frame. Moreover, $\boldsymbol{\tau}$ denotes the vector of control inputs (forces and torques), $\bar{\mathbf{M}}(\mathbf{q})$ is the positive definite inertial matrix, $\bar{\mathbf{C}}(\dot{\mathbf{q}},\mathbf{q})$ represents coriolis and centrifugal terms, $\bar{\mathbf{D}}(\dot{\mathbf{q}},\mathbf{q})$ models dissipative effects, $\bar{\mathbf{g}}(\mathbf{q})$ encapsulates the gravity and buoyancy effects. $\boldsymbol{\lambda}$ is the vector of forces and torques that exerted by the UVMS at its end-effector frame on the environment. Moreover, the dynamic equation (4) can be written in terms of task space coordinates as follows Khatib (1987):

$$\begin{aligned}\mathbf{M}(\mathbf{x_e})\ddot{\mathbf{x}}_\mathbf{e} + \mathbf{C}(\dot{\mathbf{x}}_e,\mathbf{x_e})\dot{\mathbf{x}}_\mathbf{e} + \mathbf{D}(\dot{\mathbf{x}}_\mathbf{e},\mathbf{x_e})\dot{\mathbf{x}}_\mathbf{e} \\ + \mathbf{g}(\mathbf{x_e}) + \boldsymbol{\lambda} + \mathbf{J}^\top\boldsymbol{\delta}(t) = \mathbf{u}\end{aligned} \tag{5}$$

where

$$\begin{aligned}\mathbf{M}(\mathbf{x_e}) &= \mathbf{J}^{-\top}\bar{\mathbf{M}}(\mathbf{q})\mathbf{J}^{+} \\ \mathbf{C}(\dot{\mathbf{x}}_\mathbf{e},\mathbf{x_e}) &= \mathbf{J}^{-\top}\bar{\mathbf{C}}(\dot{\mathbf{q}},\mathbf{q})\mathbf{J}_i^{+} + \mathbf{J}^{-\top}\bar{\mathbf{M}}(\mathbf{q})\dot{\mathbf{J}}^{+} \\ \mathbf{D}(\dot{\mathbf{x}}_\mathbf{e},\mathbf{x_e}) &= \mathbf{J}^{-\top}\bar{\mathbf{D}}(\dot{\mathbf{q}},\mathbf{q})\mathbf{J}^{+} \\ \mathbf{g}(\mathbf{x_e}) &= \mathbf{J}^{-\top}\bar{\mathbf{g}}(\mathbf{q})\end{aligned}$$

and $\mathbf{u} \in \mathbb{R}^6$ denotes the task space control input wrenches. It is worth mentioning that the control input vector $\boldsymbol{\tau}$, can be computed from the task space control input $\mathbf{u}$ via:

$$\boldsymbol{\tau} = \mathbf{J}^\top\mathbf{u} + (\mathbf{I}_{n\times n} - \mathbf{J}^\top\mathbf{J}^{\#\top})\boldsymbol{\tau}^0$$

where $\mathbf{J}^{\#\top} = \mathbf{J}\bar{\mathbf{M}}^{-1}[\mathbf{J}\bar{\mathbf{M}}^{-1}\mathbf{J}^{\top}]^{-1}$ is the dynamically consistent generalized inverse of the robot Jacobian Khatib (1987, 1988). The vector $\boldsymbol{\tau}^0$ is a redundancy term without contribution to the end-effector's wrench and thus can be regulated independently to achieve sub-secondary tasks.

2.3 Dynamical Systems

Consider the initial value problem:

$$\dot{\xi} = H(t,\xi), \xi(0) = \xi^0 \in \Omega_\xi, \tag{6}$$

with $H : \mathbb{R}_{\geq 0} \times \Omega_\xi \to \mathbb{R}^n$, where $\Omega_\xi \subseteq \mathbb{R}^n$ is a non-empty open set.

***Definition** 1.* (Sontag, 1998) A solution $\xi(t)$ of the initial value problem (6) is maximal if it has no proper right extension that is also a solution of (6).

***Theorem** 1.* (Sontag, 1998) Consider the initial value problem (6). Assume that $H(t,\xi)$ is: a) locally Lipschitz in ξ for almost all $t \in \mathbb{R}_{\geq 0}$, b) piecewise continuous in t for each fixed $\xi \in \Omega_\xi$ and c) locally integrable in t for each fixed $\xi \in \Omega_\xi$. Then, there exists a maximal solution $\xi(t)$ of (6) on the time interval $[0, \tau_{\max})$, with $\tau_{\max} \in \mathbb{R}_{>0}$ such that $\xi(t) \in \Omega_\xi, \forall t \in [0, \tau_{\max})$.

***Proposition** 1.* (Sontag, 1998) Assume that the hypotheses of Theorem 1 hold. For a maximal solution $\xi(t)$ on the time interval $[0, \tau_{\max})$ with $\tau_{\max} < \infty$ and for any compact set $\Omega'_\xi \subseteq \Omega_\xi$, there exists a time instant $t' \in [0, \tau_{\max})$ such that $\xi(t') \notin \Omega'_\xi$.

3. PROBLEM STATEMENT

We define here the problem that we aim to solve in this paper:

Problem 1. Given a UVMS system as well as a desired force profile that should be applied by the UVMS on an entirely unknown model compliant environment, assuming the uncertainties on the UVMS dynamic parameters, design a feedback control law such that the following are guaranteed:

(1) a predefined behavior of the system in terms of desired overshoot and prescribed transient and steady state performance.
(2) robustness with respect to the external disturbances and noise on measurement devises.

4. CONTROL METHODOLOGY

In this work we assume that the UVMS is equipped with a force/torque sensor at its end-effector frame. However, we assume that its accuracy is not perfect and the system suffers from noise in the force/torque measurements. In order to combine the features of stiffness and force control, a parallel force/position regulator is designed. This can be achieved by closing a force feedback loop around a position/velocity feedback loop, since the output of the force controller becomes the reference input to the dynamic controller of the UVMS.

4.1 Control Design

Let ${}^p\mathbf{x}_e^d \in \mathbb{R}^3$ be the reference position of the end-effector that must be reached by the end-effector's position $\mathbf{x}_e$. Also, interaction between the end-effector and a frictionless, elastically compliant environment is assumed as:

$$\mathbf{f}_e = \mathbf{K}_f({}^p\mathbf{x}_e - {}^p\mathbf{x}_e^q) \tag{7}$$

that models the compliant environment, where $\mathbf{K}_f = \text{diag}\{K_{(f,1)}, \ldots, K_{(f,3)}\} \in \mathbb{R}^{3\times 3}$ is the positive semi-definite translational stiffness matrix, which represents the elastic coefficient of the environment (see (Siciliano and Villani, 1999)), ${}^p\mathbf{x}_e^q$ is the equilibrium position of the undeformed environment which is constant w.r.t the time (i.e. ${}^p\dot{\mathbf{x}}_e^q = 0$) and $\mathbf{f}_e = [f_{e,1}, \ldots, f_{e,3}]^\top$ is already stated, the force exerted by the end-effector on the environment during the interaction. Equation (7) after time differentiation results in:

$$\dot{\mathbf{f}}_e = \mathbf{K}_f {}^p\dot{\mathbf{x}}_e \tag{8}$$

Let now $\mathbf{f}_e^d$ be the desired force corresponding to the desired end-effector position ${}^p\mathbf{x}_e^d$ (7). Hence, let us define the force error:

$$\mathbf{e}_f(t) = \mathbf{f}_e(t) + \Delta\mathbf{f}_e(t) - \mathbf{f}_e^d(t) \in \mathbb{R}^3, \tag{9}$$

where $\Delta\mathbf{f}_e(t)$ denotes the bounded noise on the force's measurement. Also we define the end-effector orientation error as:

$$\mathbf{e}_o(t) = {}^o\mathbf{x}_e(t) - {}^o\mathbf{x}_e^d(t) \in \mathbb{R}^3, \tag{10}$$

where ${}^o\mathbf{x}_e^d(t) \in \mathbb{R}^3$ is predefined desired orientation of the end-effector (e.g. ${}^o\mathbf{x}_e^d(t) = [0,\ 0,\ 0]^\top$). Now we can set the vector of desired end-effector configuration as $\mathbf{x}_e^d(t) = [\mathbf{f}_e^d(t)^\top, ({}^o\mathbf{x}_e^d(t))^\top]^\top$. Notice that the desired force $\mathbf{f}_e^d(t)$ can be related with the end-effector position via (7). In addition the overall error vector is given as:

$$\mathbf{e}_x(t) = [e_{x_1}(t), \ldots, e_{x_6}(t)] = [\mathbf{e}_f^\top(t), \mathbf{e}_o^\top(t)]^\top \tag{11}$$

A suitable methodology for the control design in hand is that of prescribed performance control, recently proposed in (Bechlioulis and Rovithakis, 2011, 2014), which is adapted here in order to achieve predefined transient and steady state response bounds for the errors. Prescribed performance characterizes the behavior where the aforementioned errors evolve strictly within a predefined region that is bounded by absolutely decaying functions of time, called performance functions. The mathematical expressions of prescribed performance are given by the inequalities: $-\rho_{x_j}(t) < e_{x_j}(t) < \rho_{x_j}(t),\ j = 1, \ldots, 6$, where $\rho_{x_j} : [t_0, \infty) \to \mathbb{R}_{>0}$ with $\rho_{x_j}(t) = (\rho_{x_j}^0 - \rho_{x_j}^\infty)e^{-l_{x_j}t} + \rho_{x_j}^\infty$ and $l_{x_j} > 0, \rho_{x_j}^0 > \rho_{x_j}^\infty > 0$, are designer specified, smooth, bounded and decreasing positive functions of time with positive parameters $l_{x_j}, \rho_{x_j}^\infty$, incorporating the desired transient and steady state performance respectively. In particular, the decreasing rate of ρ_{x_j}, which is affected by the constant l_{x_j} introduces a lower bound on the speed of convergence of e_{x_j}. Furthermore, the constants $\rho_{x_j}^\infty$ can be set arbitrarily small, achieving thus practical convergence of the errors to zeros.

Now, we propose a state feedback control protocol $\boldsymbol{u}(t)$, that does not incorporate any information regarding the UVMS dynamic model (5) and stiffens matrix $\mathbf{K}_f$, and achieves tracking of the smooth and bounded desired force trajectory $\mathbf{f}_e^d(t) \in \mathbb{R}^3$ as well as ${}^o\mathbf{x}_e^d(t)$ with an priori specified convergence rate and steady state error. Thus, given the errors (11):

Step I-a: Select the corresponding functions $\rho_{x_j}(t) = (\rho_{x_j}^0 - \rho_{x_j}^\infty)e^{-l_{x_j}t} + \rho_{x_j}^\infty$ with $\rho_{x_j}^0 > |e_{x_j}(t_0)|, \forall j \in \{1 \ldots, 6\}$

$\rho^0_{x_j} > \rho^\infty_{x_j} > 0$, $l_{x_j} > 0, \forall j \in \{1,\dots 6\}$, in order to incorporate the desired transient and steady state performance specification and define the normalized errors:

$$\xi_{x_j}(t) = \frac{e_{x_j}(t)}{\rho_{x_j}(t)},\ j = \{1,\dots,6\} \tag{12}$$

Step I-b: Define the transformed errors ε_{x_j} as:

$$\varepsilon_{x_j}(\xi_{x_j}) = \ln\Big(\frac{1+\xi_{x_j}}{1-\xi_{x_j}}\Big),\ j = \{1,\dots,6\} \tag{13}$$

Now, the reference velocity as $\dot{\mathbf{x}}^r_e = [\dot{x}^r_{e_1},\dots,\dot{x}^r_{e_6}]^\top$ is designed as:

$$\dot{x}^r_{e_j}(t) = -k_{x_j}\varepsilon_{x_j}(\xi_{x_j}),\ k_j > 0,\ j = \{1,\dots,6\} \tag{14}$$

Step II-a: Define the velocity error vector at the end-effector frame as:

$$\mathbf{e}_v(t) = [e_{v_1}(t),\dots,e_{v_6}(t)]^\top = \dot{\mathbf{x}}_e(t) - \dot{\mathbf{x}}^r_e(t) \tag{15}$$

and select the corresponding functions $\rho_{v_j}(t) = (\rho^0_{v_j} - \rho^\infty_{v_j})e^{-l_{v_j}t} + \rho^\infty_{v_j}$ with $\rho^0_{v_j} > |e_{v_j}(t_0)|, \forall j \in \{1\dots,6\}$, $\rho^0_{v_j} > \rho^\infty_{v_j} > 0$, $l_{v_j} > 0, \forall j \in \{1,\dots 6\}$, and define the normalized velocity errors $\boldsymbol{\xi}_v$ as:

$$\boldsymbol{\xi}_v(t) = [\xi_{v_1},\dots,\xi_{v_6}]^\top = \mathbf{P}^1_v(t)\mathbf{e}_v(t) \tag{16}$$

where $\mathbf{P}^1_v(t) = \mathrm{diag}\{\rho_{v_j}\}, j \in \{1,\dots,6\}$.

Step II-b: Define the transformed errors $\boldsymbol{\varepsilon}_v(\boldsymbol{\xi}_v) = [\varepsilon_{v_1}(\xi_{v_1}),\dots,\varepsilon_{v_6}(\xi_{v_6})]^\top$ and the signal $\mathbf{R}_v(\boldsymbol{\xi}_v) = \mathrm{diag}\{r_{v_j}\}$, $j \in \{1,\dots,6\}$ as:

$$\boldsymbol{\varepsilon}_v(\boldsymbol{\xi}_v) = \Big[\ln\Big(\frac{1+\xi_{v_1}}{1-\xi_{v_1}}\Big),\dots,\ln\Big(\frac{1+\xi_{v_6}}{1-\xi_{v_6}}\Big)\Big]^\top \tag{17}$$

$$\mathbf{R}_v(\boldsymbol{\xi}_v) = \mathrm{diag}\{r_{v_j}(\xi_{v_j})\} = \mathrm{diag}\Big\{\frac{2}{1-\xi^2_{v_j}}\Big\}, j = \{1,\dots,6\} \tag{18}$$

and finally design the state feedback control law $u_j,\ j \in \{1,\dots,6\}$ as:

$$u_j(\xi_{xj},\xi_{vj},t) = -k_{v_j}\frac{r_{v_j}(\xi_{v_j})\varepsilon_{v_j}(\xi_{v_j})}{\rho_{v_j}(t)},\ j = \{1,\dots,6\} \tag{19}$$

where k_{v_j} to be a positive gain. The control law (19) can be written in vector form as:

$$\begin{aligned}\mathbf{u}(\mathbf{e}_x(t),\mathbf{e}_v(t),t) = {}& [u_1(\xi_{x_1},\xi_{v_1},t),\dots,u_6(\xi_{x_6},\xi_{v_6},t)]^\top \\ & - \mathbf{K}_v\mathbf{P}^{-1}(t)\mathbf{R}_v(\boldsymbol{\xi}_v)\boldsymbol{\varepsilon}_v(\boldsymbol{\xi}_v)\end{aligned} \tag{20}$$

with $\mathbf{K}_v$ to be the diagonal matrix containing k_{v_j}. Now we are ready to state the main theorem of the paper:

***Theorem** 2.* Given the error defined in (11) and the required transient and steady state performance specifications, select the exponentially decaying performance function $\rho_{x_j}(t)$, $\rho_{v_j}(t)$ such that the desired performance specifications are met. Then the state feedback control law of (20) guarantees tracking of the trajectory $\mathbf{f}^d_e(t) \in \mathbb{R}^3$ as well as ${}^o\mathbf{x}^d_e(t)$:

$$\lim_{t\to\infty}\mathbf{f}_e(t) = \mathbf{f}^d_e(t) \text{ and } \lim_{t\to\infty}{}^o\mathbf{x}_e(t) = {}^o\mathbf{x}^d_e(t)$$

with the desired transient and steady state performance specifications.

Proof. For the proof we follow parts of the approach in (Bechlioulis and Rovithakis, 2014). We start by differentiating (12) and (16) with respect to the time and substituting the system dynamics (5) as well as (14) and (19) and employing (11) and (15), obtaining:

$$\begin{aligned}\dot{\xi}_{x_j}(\xi_{x_j},t) &= h_{x_j}(\xi_{x_j},t) \\ &= \rho^{-1}_{x_j}(t)(\dot{e}_{x_j}(t) - \dot{\rho}_{x_j}(t)\xi_{x_j}) \\ &= \rho^{-1}_{x_j}(t)(-k_{x_j}\varepsilon_{x_j}(\xi_{x_j}) + \xi_{v_j}\rho_{v_j}(t) - \dot{x}^d_{e_j}(t)) \\ &\quad - \rho^{-1}_{x_j}(t)(\dot{\rho}_{x_j}(t)\xi_{x_j}), \forall j \in \{1,\dots,6\}\end{aligned} \tag{21}$$

$$\begin{aligned}\dot{\boldsymbol{\xi}}_v(\xi_v,t) &= h_v(\xi_v,t) \\ &= \mathbf{P}^{-1}_v((\ddot{\mathbf{x}}_e - \ddot{\mathbf{x}}^d_e) - \dot{\mathbf{P}}^{-1}_v\dot{\boldsymbol{\xi}}_v) \\ &= -\mathbf{K}_v\mathbf{P}^{-1}_v\mathbf{M}^{-1}\mathbf{P}^{-1}_v\mathbf{R}_v\boldsymbol{\varepsilon}_v - \\ &\quad - \mathbf{P}^{-1}_v\Big[\mathbf{M}^{-1}\Big(\mathbf{C}\cdot(\mathbf{P}_v\boldsymbol{\xi}_v + \dot{\mathbf{x}}^r_e) + \mathbf{D}\cdot(\mathbf{P}_v\boldsymbol{\xi}_v + \dot{\mathbf{x}}^r_e) \\ &\quad + \mathbf{g} + \boldsymbol{\lambda} + \mathbf{J}^\top\boldsymbol{\delta}(t)\Big) + \dot{\mathbf{P}}_v\boldsymbol{\xi}_v + \frac{\partial}{\partial t}\dot{\mathbf{x}}^r_e\Big]\end{aligned} \tag{22}$$

Now let us to define the vectors of normalized state error and the generalized normalized error as $\boldsymbol{\xi}_x = [\xi_{x_1},\dots,\xi_{x_6}]^\top$, and $\boldsymbol{\xi} = [\boldsymbol{\xi}^\top_x, \boldsymbol{\xi}^\top_v]^\top$, respectively. The equations of (21) and (22) now can be written in compact form as:

$$\dot{\boldsymbol{\xi}} = h(\boldsymbol{\xi},t) = [h^\top_v(\xi_v,t), h^\top_v(\xi_v,t)] \tag{23}$$

Let us define the open set $\Omega_\xi = \Omega_{\xi_x} \times \Omega_{\xi_v}$ with $\Omega_{\xi_x} = \Omega_{\xi_v} = (-1,1)^6$. In what follows, we proceed in two phases. First we ensure the existence of a unique maximal solution $\boldsymbol{\xi}(t)$ of (23) over the set Ω_ξ for a time interval $[0,t_{\max}]$ (i.e., $\boldsymbol{\xi}(t) \in \Omega_\xi, \forall t \in [0,t_{\max}]$). Then, we prove that the proposed controller (20) guarantees, for all $t \in [0,t_{\max}]$ the boundedness of all closed loop signal of (23) as well as that $\boldsymbol{\xi}(t)$ remains strictly within the set Ω_ξ, which leads that $t_{\max} = \infty$ completes the proof.

Phase A: The set Ω_ξ is nonempty and open, thus by selecting $\rho^0_{x_j} > |e_{x_j}(0)|$ and $\rho^0_{v_j} > |e_{v_j}(0)|$, $\forall j \in \{1,\dots 6\}$ we guarantee that $\boldsymbol{\xi}_x(0) \in \Omega_x$ and $\boldsymbol{\xi}_v(0) \in \Omega_v$. Additionally, h is continuous on t and locally Lipschitz on $\boldsymbol{\xi}$ over Ω_ξ. Therefore, the hypotheses of Theorem1 hold and the existence of a maximal solution $\boldsymbol{\xi}(t)$ of (23) on a time interval $[0,t_{\max}]$ such that $\boldsymbol{\xi}(t) \in \Omega_\xi,\ \forall t \in [0,t_{\max}]$ is ensured.

Phase B: In the Phase A we have proven that $\boldsymbol{\xi}(t) \in \Omega_\xi,\ \forall t \in [0,t_{\max}]$, thus it can be concluded that:

$$\xi_{c_j}(t) = \frac{e_{c_j}}{\rho_{c_j}} \in (-1,1),\ \forall j\{1,\dots,6\},\ c \in \{x,v\} \tag{24}$$

for all $t \in [0,t_{\max}]$, from which we obtain that $e_{x_j}(t)$ and $e_{v_j}(t)$ are absolutely bounded by ρ_{x_j} and ρ_{v_j}, respectively. Therefore, the error vectors $\varepsilon_{x_j}(\xi_{x_j}), \forall j \in \{1,\dots,6\}$ and $\varepsilon_{v_j}(\xi_{v_j}), \forall j \in \{1,\dots,6\}$ defined in (13) and (18), respectively, are well defined for all $t \in [0,t_{\max}]$. Hence, consider the positive definite and radially unbounded functions $V_{x_j}(\varepsilon_{x_j}) = \varepsilon^2_{x_j},\ \forall j\{1,\dots,6\}$. Differentiating of V_{x_j} w.r.t time and substituting (21), results in:

$$\dot{V}_{x_j} = -\frac{4\varepsilon_{x_j}}{(1-\xi^2_{x_j})\rho_{x_j}}\Big(k_{x_j}\varepsilon_{x_j}(\xi_{x_j}) + \dot{x}^d_{e_j} + \dot{\rho}_{x_j}(t)\xi_{x_j} - \rho_{v_j}(t)\xi_{v_j}\Big) \tag{25}$$

since $\dot{x}^d_{e_j}$,ρ_{x_j},ρ_{v_j} are bounded by construction and ξ_{x_j},ξ_{v_j} are bounded in $(-1,1)$, owing to (24), $\dot{V}_{x_j}$ becomes:

$$\dot{V}_{x_j} = -\frac{4}{(1-\xi^2_{x_j})\rho_{x_j}}\Big(B_x|\varepsilon_{x_j}| - k_{x_j}|\varepsilon_{x_j}|^2\Big) \tag{26}$$

$\forall t \in [0,t_{\max}]$, where B_x is an unknown positive constant independent of $t_{\max}$ satisfying $B_x > |\dot{x}^d_{e_j} + \dot{\rho}_{x_j}(t)\xi_{x_j} -$

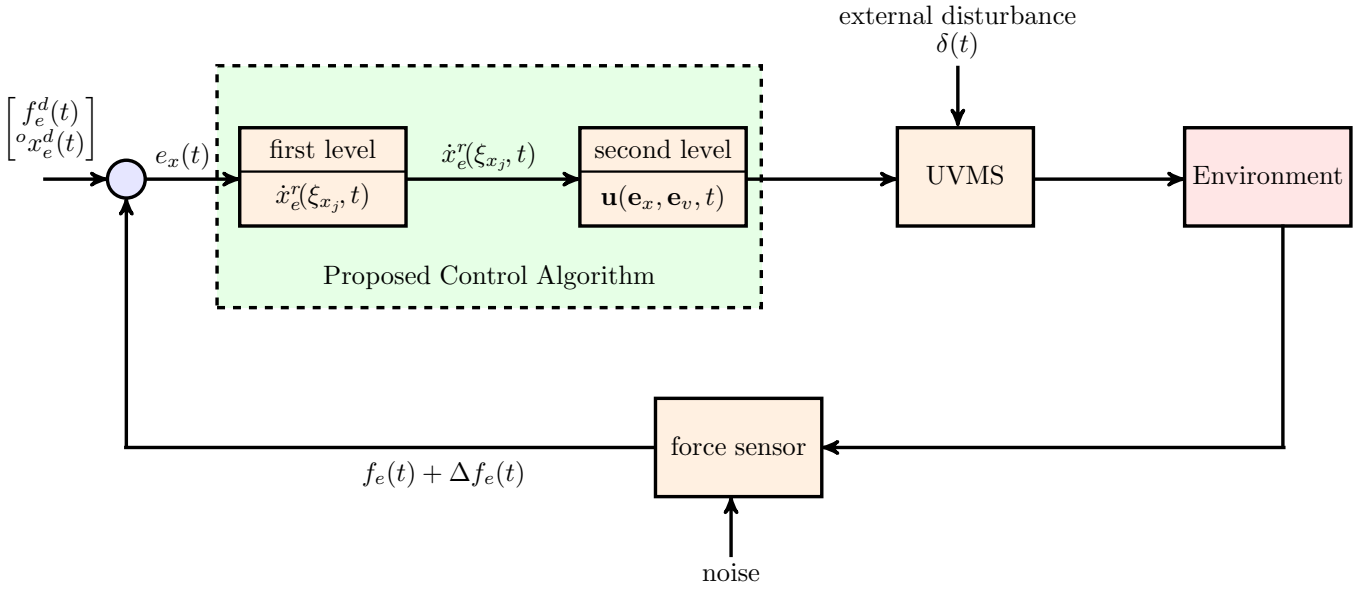

Fig. 1. The closed loop block diagram of the proposed control scheme.

$\rho_{v_j}(t)\xi_{v_j}|$. Therefore, we conclude that $\dot{V}_{x_j}$ is negative when $\varepsilon_{x_j} > \frac{B_x}{k_{j_x}}$ and subsequently that

$$|\varepsilon_{x_j}(\xi_{x_j}(t))| \leq \bar{\varepsilon}_{x_j} = \max\{\varepsilon_{x_j}(\xi_{x_j}(0)), \frac{B_x}{k_{j_x}}\} \tag{27}$$

$\forall t \in [0, t_{\max}], \forall j\{1, \ldots, 6\}$. Furthermore, from (13), taking the inverse logarithm, we obtain:

$$-1 < \frac{e^{-\bar{\varepsilon}_{x_j}} - 1}{e^{-\bar{\varepsilon}_{x_j}} + 1} = \underline{\xi}_{x_j} \leq \xi_{x_j}(t) \leq \bar{\xi}_{x_j} = \frac{e^{\bar{\varepsilon}_{x_j}} - 1}{e^{\bar{\varepsilon}_{x_j}} + 1} < 1 \tag{28}$$

$\forall t \in [0, t_{\max}],\ j \in \{1, \ldots, 6\}$. Due to (28), the reference velocity vector $\dot{\mathbf{x}}_e^r$ as defined in (14), remains bounded for all $t \in [0, t_{\max}]$. Moreover, invoking $\dot{\mathbf{x}}_e = \dot{\mathbf{x}}_e^r(t) + \mathbf{P}_v(t)\xi_v$ from (15), (16) and (24), we also conclude the boundedness of $\dot{\mathbf{x}}_e$ for all $t \in [0, t_{\max}]$. Finally, differentiating $\dot{\mathbf{x}}_e^r(t)$ w.r.t time and employing (21), (24) and (28), we conclude the boundedness of $\frac{\partial}{\partial t}\dot{\mathbf{x}}_e^r(t)$, $\forall t \in [0, t_{\max}]$. Applying the aforementioned line of proof, we consider the positive definite and radially unbounded function $V_v(\varepsilon_v) = \frac{1}{2}||\varepsilon||^2$. By differentiating V_v with respect to time, substituting (22) and by employing continuity of $\mathbf{M}$, $\mathbf{C}$, $\mathbf{D}$, $\mathbf{g}$, $\boldsymbol{\lambda}$, $\boldsymbol{\delta}$, $\boldsymbol{\xi_x}$, $\boldsymbol{\xi_v}$,$\dot{\mathbf{P}}_v$, $\frac{\partial}{\partial t}\dot{\mathbf{x}}_e^r$, $\forall t \in [0, t_{\max}]$, we obtain:

$$\dot{V}_v \leq ||\mathbf{P}_v^{-1}\mathbf{R}_v(\boldsymbol{\xi}_v)\boldsymbol{\varepsilon}_v||\Big(B_v - \mathbf{K}_v\lambda_M||\mathbf{P}_v^{-1}\mathbf{R}_v(\boldsymbol{\xi}_v)\boldsymbol{\varepsilon}_v||\Big)$$

$\forall t \in [0, t_{\max}]$, where λ_M is the minimum singular value of the positive definite matrix $\mathbf{M}^-1$ and B_v is a positive constant independent of $t_{\max}$, satisfying

$$B_v \geq ||\mathbf{M}^{-1}\Big(\mathbf{C}\cdot(\mathbf{P}_v\boldsymbol{\xi}_v + \dot{\mathbf{x}}_e^r(t)) + \mathbf{D}\cdot(\mathbf{P}_v\boldsymbol{\xi}_v + \dot{\mathbf{x}}_e^r(t)) + \mathbf{g} + \boldsymbol{\lambda} + \mathbf{J}^\top\boldsymbol{\delta}(t) + \dot{\mathbf{P}}_v\boldsymbol{\xi}_v + \frac{\partial}{\partial t}\dot{\mathbf{x}}_e^r\Big)||$$

Thus, $\dot{V}_v$ is negative when $||\mathbf{P}_v^{-1}\mathbf{R}_v(\boldsymbol{\xi}_v)\boldsymbol{\varepsilon}_v|| > B_v(\mathbf{K}_v\lambda_M)^{-1}$, which by employing the definitions of $\mathbf{P}_v$ and $\mathbf{R}_v$, becomes $||\boldsymbol{\varepsilon}_v|| > B_v(\mathbf{K}_v\lambda_M)^{-1}\max\{\rho_{v_1}^0, \ldots, \rho_{v_6}^0\}$. Therefore, we conclude that:

$$||\boldsymbol{\varepsilon}_v(\boldsymbol{\xi}_v(t)) \leq \bar{\boldsymbol{\varepsilon}}_v = \max\Big\{\boldsymbol{\varepsilon}_v(\boldsymbol{\xi}_v(0)), B_v(\mathbf{K}_v\lambda_M)^{-1}\cdot\max\{\rho_{v_1}^0, \ldots, \rho_{v_6}^0\}\Big\}$$

$\forall t \in [0, t_{\max}]$. Furthermore, from (18), invoking that $|\varepsilon_{v_j}| \leq ||\boldsymbol{\varepsilon}_v||$, we obtain:

$$-1 < \frac{e^{-\bar{\varepsilon}_{v_j}} - 1}{e^{-\bar{\varepsilon}_{v_j}} + 1} = \underline{\xi}_{v_j} \leq \xi_{v_j}(t) \leq \bar{\xi}_{v_j} = \frac{e^{\bar{\varepsilon}_{v_j}} - 1}{e^{\bar{\varepsilon}_{v_j}} + 1} < 1 \tag{29}$$

$\forall t \in [0, t_{\max}],\ j \in \{1, \ldots, 6\}$ which also leads to the boundedness of the control law (20). Now, we will show that the $t_{\max}$ can be extended to ∞. Obviously, notice by (28) and (29) that $\boldsymbol{\xi}(t) \in \Omega_\xi^{'} = \Omega_{\xi_x}^{'} \times \Omega_{\xi_v}^{'}, \forall t \in [0, t_{\max}]$, where:

$$\Omega_{\xi_c}^{'} = [\underline{\xi}_{c_1}, \bar{\xi}_{c_1}] \times \ldots, \times [\underline{\xi}_{c_6}, \bar{\xi}_{c_6}],\ c \in \{x, v\}$$

are nonempty and compact subsets of Ω_{ξ_x} and Ω_{ξ_v}, respectively. Hence, assuming that $t_{\max} < \infty$ and since $\Omega_\xi \subset \Omega_\xi^{'}$, Proposition 1, dictates the existence of a time instant $t^{'} \in \forall t \in [0, t_{\max}]$ such that $\boldsymbol{\xi}(t^{'}) \notin \Omega_\xi^{'}$, which is a clear contradiction. Therefore, $t_{\max} = \infty$. Thus, all closed loop signals remain bounded and moreover $\boldsymbol{\xi}(t) \in \Omega_\xi^{'}, \forall t \geq 0$. Finally, from (12) and (28) we conclude that:

$$-\rho_{x_j} < \frac{e^{-\bar{\varepsilon}_{x_j}} - 1}{e^{-\bar{\varepsilon}_{x_j}} + 1}\rho_{x_j} \leq e_{x_j}(t) \leq \rho_{x_j}\frac{e^{\bar{\varepsilon}_{x_j}} - 1}{e^{\bar{\varepsilon}_{x_j}} + 1} < \rho_{x_j} \tag{30}$$

for $j \in \{1, \ldots, 6\}$ and for all $t \geq 0$ and consequently, completes the proof.

Remark 1. From the aforementioned proof, it is worth noticing that the proposed control scheme is model free with respect to the matrices $\mathbf{M}$, $\mathbf{C}$, $\mathbf{D}$, $\mathbf{g}$ as well as the external disturbances $\boldsymbol{\delta}$ that affect only the size of $\bar{\varepsilon}_{c_j}, c \in \{x, v\}$ but leave unaltered the achieved convergence properties as (30) dictates. In fact, the actual transient and steady state performance is determined by the selection of the performance function $\rho_{c_j}, c \in \{x, v\}$. Finally the closed loop block diagram of the proposed control scheme is indicated in Fig.1.

5. SIMULATION RESULTS

A simulation study was conducted employing a dynamic simulator built in MATLAB. The dynamic equation of

UVMS used in this simulator is derived following Schjlberg and Fossen (1994). The UVMS model considered in the simulations is the SeaBotix LBV150 equipped with a 4 DoF manipulator. We consider a scenario involving 3D motion in workspace, where the end-effector of the UVMS is in interaction on a compliant environment with stiffens matrix $\mathbf{K}_f = \text{diag}\{2\}$ which is unknown for the controller. The workspace at the initial time, including

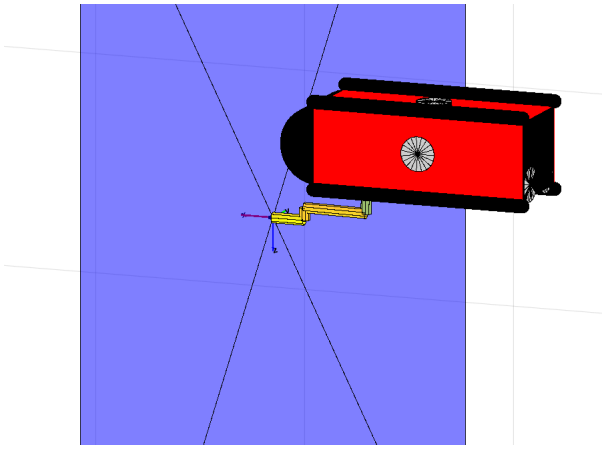

Fig. 2. Workspace including the UVMS and the compliant environment. The UVMS is run under the influence of external disturbances.

UVMS and the compliant environment are depicted in Fig.2. More specifically, we adopt: $\mathbf{f}_e(0) = [0,0,0]^\top$ and ${}^o\mathbf{x}_e = [0.2, 0.2, -0.2]^\top$. It means that at the initial time of the simulation study we assume that the uvms has attached the compliant environment with a rotation at its end-effector frame. The control gains for the two set of the simulation studies were selected as follows: $k_{x_j} = -0.2j \in \{1,\dots,6\}$, $k_{v_j} = -5j \in \{1,\dots,6\}$. Moreover, the dynamic parameters of UVMSs as well as the stiffens matrix $\mathbf{K}_f$ were considered unknown for the controller. The parameters of the performance functions in sequel stimulation studies were chosen as follows: $\rho^0_{x_1} = 2$, $\rho^0_{x_j} = 1$, $j \in \{2,3\}$, $\rho^0_{x_j} = 0.4$, $j \in \{4,5,6\}$, $\rho^0_{v_j} = 2$, $j \in \{1,2,3\}$, $\rho^0_{v_j} = 1$, $j \in \{4,5,6\}$, $\rho^\infty_{x_j} = 0.05$ $j \in \{1,\dots,6\}$, $\rho^\infty_{v_j} = 0.15$ $j \in \{1,\dots,6\}$, $l_{x_j} = 6$ $j \in \{1,2,3\}$, $l_{x_j} = 2$ $j \in \{4,5,6\}$, $l_{v_j} = 4$ $j \in \{1,2,3\}$, $l_{v_j} = 2.5$ $j \in \{4,5,6\}$. Finally, the whole system was running under the influence of external disturbances (e.g., sea current) acting along x and y axis (on the vehicle body) and bounded at 0.1 N, in order to test the robustness of the proposed scheme. Moreover, bounded noise on measurement devices were considered during the simulation study.

Two set of simulation studies are presented here. In the first scenario, a constant desired force should be exerted to the environment while predefined orientation must be kept. The desired constant force and the orientation are $\mathbf{f}^d_e = [0.6, 0, 0]^\top$ and ${}^o\mathbf{x}^d_e = [0.0, 0.0, 0.0]^\top$ respectively. The results are depicted in Figs 3-4. The evolution of the errors at the first and second level of the proposed controller are indicated in Fig.3 and Fig.4, respectively. It can be concluded that even with the influence of external disturbances as well as noise in measurements, the errors in all directions converge close to zero and remain bounded by the performance functions.

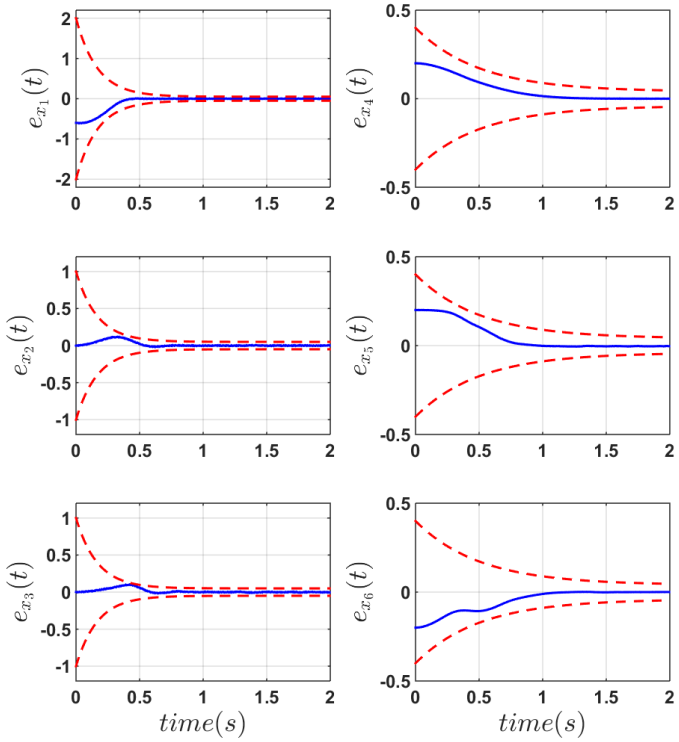

Fig. 3. Constant scenario: The evolution of the errors at the first level of the proposed control scheme. The errors and performance bounds are indicated by blue and red color respectively.

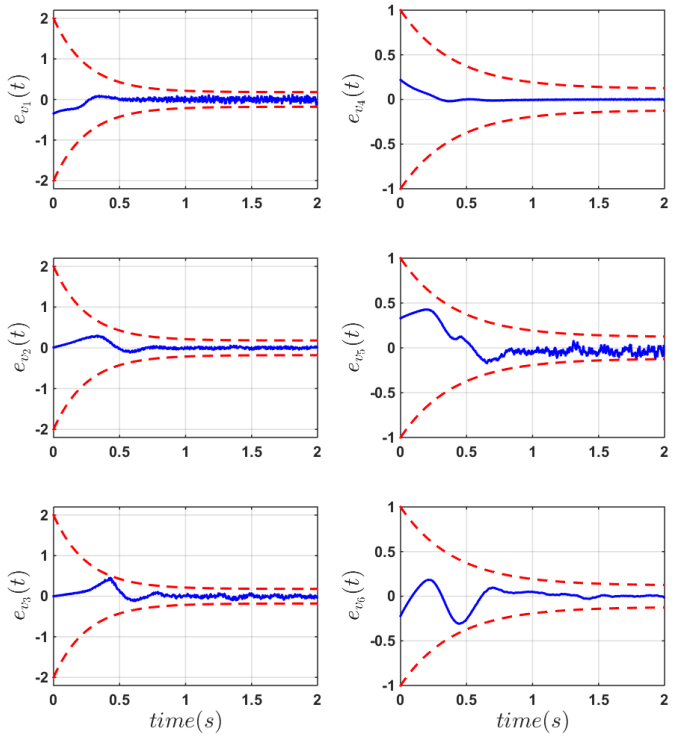

Fig. 4. Constant scenario: The evolution of the errors at the second level of the proposed control scheme. The errors and performance bounds are indicated by blue and red color respectively.

In the second simulation scenario, tracking of a desired force trajectory on the compliant environment is presented. One should bear in mind that this is a challenging task because of the dynamic nature of the underwater environment. The UVMS's model uncertainties and external disturbances in this case can easily cause unpredicted instabilities to the system. The desired force trajectory considered in this simulations is $f_{e_1}^d = 0.3\sin(\frac{2\pi}{2}t) + .3$. The results is depicted in Figs 5-7. Again, it can be seen

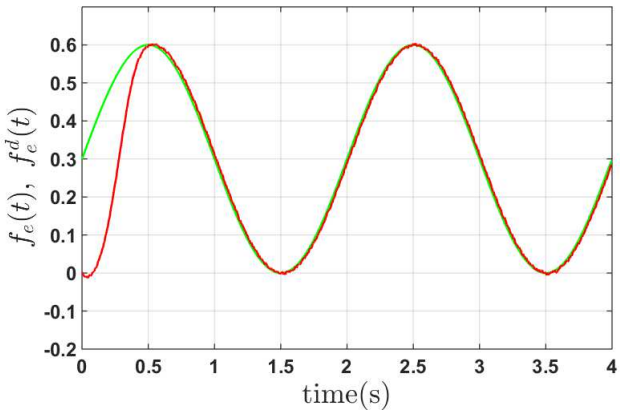

Fig. 5. Trajectory scenario: The evolution of the force trajectory. The desired force trajectory and the actual force exerted by the UVMS are indicated by green and red color respectively.

that the errors in all directions converge close to zero and remain bounded by the performance functions. Fig5 show the evolution of the force trajectory. Obviously, the actual force exerted by the UVMS (indicated by red color) converges to the desired one (indicated by green color) without overshooting and follows the desired force profile. Finally this work is accompanied by a video demonstrating the aforementioned simulation study which can be also found in HD quality at: `https://youtu.be/klKatFAADHM`

6. CONCLUSIONS AND FUTURE WORK

This work presents a robust force/position control scheme for a UVMS in interaction with a compliant environment, which could have direct applications in the underwater robotics (e.g. sampling of the sea organisms, underwater welding, pushing a button). Our proposed control scheme does not required any priori knowledge of the UVMS dynamical parameters as well as environment model. It guarantees a predefined behavior of the system in terms of desired overshot and transient and steady state performance. Moreover, the proposed control scheme is robust with respect to the external disturbances and measurement noises. The proposed controller of this work exhibits the following important characteristics: i) it is of low complexity and thus it can be used effectively in most of today UVMS. ii) The performance of the proposed scheme (e.g. desired overshot, steady state performance of the systems) is a priori and explicitly imposed by certain designer-specified performance functions, and is fully decoupled by the control gains selection, thus simplifying the control design. The simulations results demonstrated the efficiency of the proposed control scheme. Finally, future

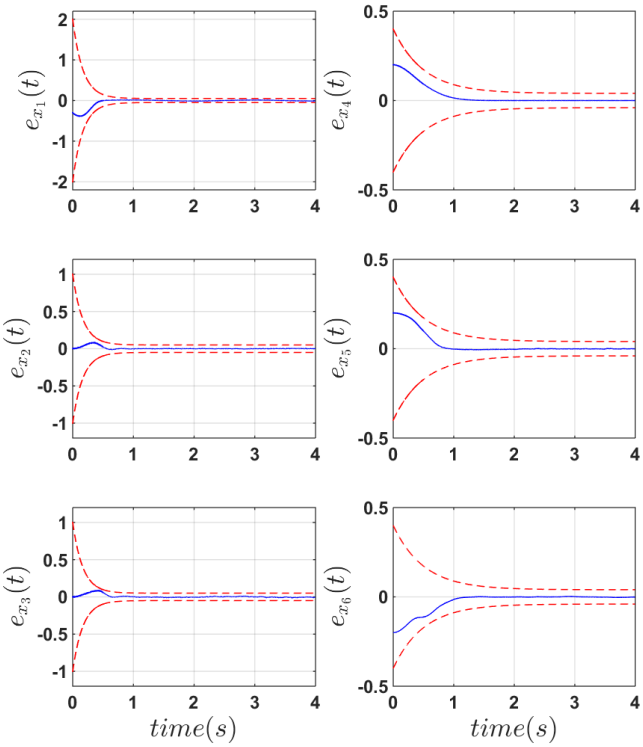

Fig. 6. Trajectory scenario: The evolution of the errors at the first level of the proposed control scheme. The errors and performance bounds are indicated by blue and red color respectively.

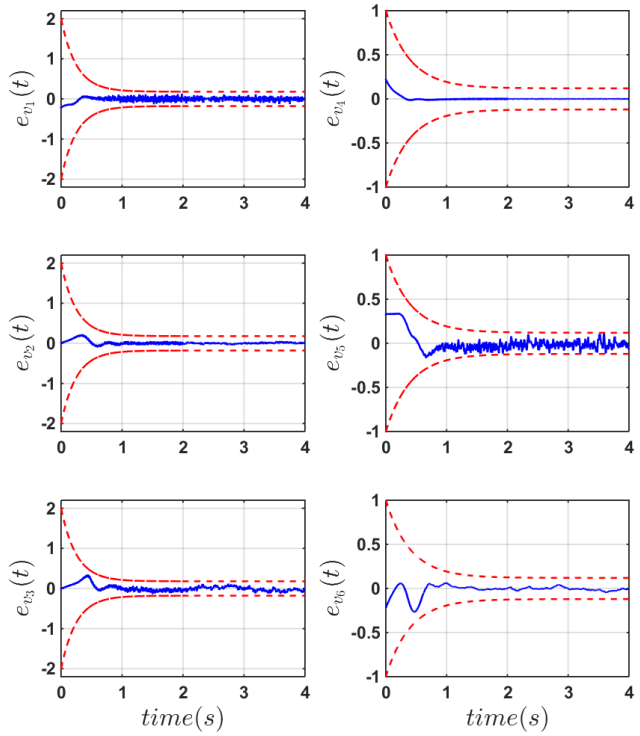

Fig. 7. Trajectory scenario: The evolution of the errors at the second level of the proposed control scheme. The errors and performance bounds are indicated by blue and red color respectively.

research efforts will be devoted towards addressing the torque controller as well as conducting experiments with a real UVMS system.

REFERENCES

Antonelli, G. (2013). *"Underwater Robots"*. Springer Tracts in Advanced Robotics. Springer International Publishing.

Antonelli, G., Sarkar, N., and Chiaverini, S. (1999). External force control for underwater vehicle-manipulator systems. In *Decision and Control, 1999. Proceedings of the 38th IEEE Conference on*, volume 3, 2975–2980 vol.3.

Antonelli, G., Sarkar, N., and Chiaverini, S. (2002). Explicit force control for underwater vehicle-manipulator systems. *Robotica*, 20(3), 251–260.

Antonelli, G., Chiaverini, S., and Sarkar, N. (2001). External force control for underwater vehicle-manipulator systems. *Robotics and Automation, IEEE Transactions on*, 17(6), 931–938.

Bechlioulis, C.P. and Rovithakis, G.A. (2011). Robust partial-state feedback prescribed performance control of cascade systems with unknown nonlinearities. *IEEE Transactions on Automatic Control*, 56.

Bechlioulis, C. and Rovithakis, G. (2014). A low-complexity global approximation-free control scheme with prescribed performance for unknown pure feedback systems. *Automatica*, 50(4), 1217–1226.

Carrera, A., Palomeras, N., Hurtos, N., Kormushev, P., and Carreras, M. (2015). Learning multiple strategies to perform a valve turning with underwater currents using an i-auv. *MTS/IEEE OCEANS 2015 - Genova: Discovering Sustainable Ocean Energy for a New World*.

Carrera, A., Palomeras, N., Ribas, D., Kormushev, P., and Carreras, M. (2014). An intervention-auv learns how to perform an underwater valve turning. *OCEANS 2014 - TAIPEI*.

Casalino, G., Angeletti, D., Bozzo, T., and Marani, G. (2001). Dexterous underwater object manipulation via multirobot cooperating systems. *Proceedings - IEEE International Conference on Robotics and Automation*, 4, 3220–3225.

Cataldi, E. and Antonelli, G. (2015). Basic interaction operations for an underwater vehicle-manipulator system. *Proceedings of the 17th International Conference on Advanced Robotics, ICAR 2015*, 524–529.

Clegg, A., Dunnigan, M., and Lane, D. (2001). Self-tuning position and force control of an underwater hydraulic manipulator. *Robotics and Automation, 2001. Proceedings 2001 ICRA. IEEE International Conference on*, 4, 3226–3231 vol.4.

Cui, Y., Podder, T., and Sarkar, N. (1999). Impedance Control of Underwater Vehicle-Manipulator Systems (uvms). *IEEE/RSJ International Conference on Intelligent Robots and Systems*, 148–153 vol.1.

Cui, Y. and Sarkar, N. (2000). A unified force control approach to autonomous underwater manipulation. *Robotics and Automation, 2000. Proceedings. ICRA '00. IEEE International Conference on*, 2, 1263–1268 vol.2.

Cui, Y. and Yuh, J. (2003). A unified adaptive force control of underwater vehicle-manipulator systems (uvms). In *Intelligent Robots and Systems, 2003. (IROS 2003). Proceedings. 2003 IEEE/RSJ International Conference on*, volume 1, 553–558 vol.1. doi:10.1109/IROS.2003.1250687.

Dunnigan, M., Lane, D., Clegg, A., and Edwards, I. (1996). Hybrid position/force control of a hydraulic underwater manipulator. *Control Theory and Applications, IEE Proceedings -*, 143(2), 145–151.

Farivarnejad, H. and Moosavian, S.A.A. (2014). Multiple impedance control for object manipulation by a dual arm underwater vehiclemanipulator system. *Ocean Engineering*, 89(0), 82 – 98.

Fernndez, J., Prats, M., Sanz, P., Garca, J., Marn, R., Robinson, M., Ribas, D., and Ridao, P. (2013). Grasping for the seabed: Developing a new underwater robot arm for shallow-water intervention. *IEEE Robotics and Automation Magazine*, 20(4), 121–130.

Fossen, T. (1994). Guidance and control of ocean vehicles. *Wiley, New York*.

Kajita, H. and Kosuge, K. (1997). Force control of robot floating on the water utilizing vehicle restoring force. *Intelligent Robots and Systems, 1997. IROS '97., Proceedings of the 1997 IEEE/RSJ International Conference on*, 1, 162–167 vol.1.

Khatib, O. (1987). A unified approach for motion and force control of robot manipulators: The operational space formulation. *IEEE Journal on Robotics and Automation*, 3(1), 43–53.

Khatib, O. (1988). Object manipulation in a multi-effector robot system. *in proceeding of the 4th International Symposium on Robotic Research*, 4, 137–144.

Lapierre, L., Fraisse, P., and Dauchez, P. (2003). Position/force control of an underwater mobile manipulator. *Journal of Robotic Systems*, 20(12), 707–722.

Marani, G., Choi, S., and Yuh, J. (2010). Real-time center of buoyancy identification for optimal hovering in autonomous underwater intervention. *Intelligent Service Robotics*, 3(3), 175–182.

Prats, M., Ribas, D., Palomeras, N., Garca, J., Nannen, V., Wirth, S., Fernndez, J., Beltrn, J., Campos, R., Ridao, P., Sanz, P., Oliver, G., Carreras, M., Gracias, N., Marn, R., and Ortiz, A. (2012). Reconfigurable auv for intervention missions: A case study on underwater object recovery. *Intelligent Service Robotics*, 5(1), 19–31.

Schjlberg, I. and Fossen, T.I. (1994). Modelling and control of underwater vehicle-manipulator systems. *in Proc. rd Conf. on Marine Craft maneuvering and control*, 45–57.

Siciliano, B., Sciavicco, L., and Villani, L. (2009). Robotics: modelling, planning and control. *Springer Verlag*.

Siciliano, B. and Villani, L. (1999). *Robot Force Control*. Kluwer international series in engineering and computer science: Robotics: vision, manipulation and sensors.

Simetti, E., Casalino, G., Torelli, S., Sperind, A., and Turetta, A. (2014). Floating underwater manipulation: Developed control methodology and experimental validation within the trident project. *Journal of Field Robotics*, 31(3), 364–385.

Sontag, E.D. (1998). *Mathematical Control Theory*. Springer, London, U.K.